Journal of Oleo Science
Copyright ©2017 by Japan Oil Chemists' Society
doi : 10.5650/jos.ess16204
J. Oleo Sci. **66**, *(5) 443-454 (2017)*

A Novel Chemical Enhancer Approach for Transdermal Drug Delivery with C_{17}-Monoglycerol Ester Liquid Crystal-forming Lipid

Wesam R. Kadhum[1], Shohei Sekiguchi[1], Ichiro Hijikuro[2], Hiroaki Todo[1] and Kenji Sugibayashi[1]*

[1] *Faculty of Pharmaceutical Sciences, Josai University, 1-1 Keyakidai, Sakado, Saitama 350-0295, JAPAN*
[2] *Farnex Incorporated, Tokyo Institute of Technology Yokohama Venture Plaza, 4259 3. Nagatsuta-cho, Midori-ku, Yokohama Kanagawa 226-8510, JAPAN*

Abstract: Transdermal administration of drugs represents an excellent alternative to conventional pharmaceutical dosage forms. However, insufficient penetration of the active pharmaceutical substance through the skin is a common problem. Thus, in the present study we evaluated the skin permeation enhancing ability of liquid crystal (LC) topical formulations. A recently developed LC-forming lipid, C_{17}-monoglycerol ester (MGE), was evaluated and compared with glycerol monoolate (GMO), which is considered as the gold standard for LC formulations. We initially prepared LC formulations containing drugs with different physiochemical properties (tranexamic acid [TXA], 4-methoxy-salicylic acid [4-MS], catechin [CC], and calcein [Cal]), and confirmed the LC phase structures in the prepared formulations using a polarizing light microscope and a small-angle X-ray scattering (SAXS). The physicochemical properties of these formulations were also assessed using a viscometer and a zetasizer. The release rate of the drugs from the LC formulations was determined using a dialysis release method. The skin penetration-enhancing ability of LC formulations was also investigated in an *in vitro* skin permeation study. The results showed that both MGE- and GMO-LC-forming lipids shared the same behavior in terms of their birefringence indexes, LC phase structures, particle sizes, and zeta potentials. Both the MGE- and GMO-LC formulations managed to improve the skin permeation for various drugs with a range of physiochemical properties. However, MGE formulations showed lower viscosity, faster drug release rate, and better skin penetration-enhancing ability than GMO formulations, strongly suggesting that the low viscosity of MGE-LC-forming lipids might influence drug diffusivity and permeability through the skin. The present MGE-LC formulation might be utilized as a promising new topical formulation for therapeutic drugs and cosmetic ingredients.

Key words: liquid crystal, C_{17}-monoglycerol ester, glycerol monoolate, topical formulations, skin penetration

1 Introduction

Transdermal administration of drugs represents an excellent alternative to conventional pharmaceutical dosage forms. Transdermal delivery provides convenient and pain-free self-administration for patients. It eliminates frequent dosing administration and peaks and troughs in plasma level associated with oral dosing and injections to maintain a constant drug concentration, so that drugs with a short half-life can be delivered effectively. However, transdermal drug delivery often faces the problem of no or insufficient penetration of the active pharmaceutical substance through the skin. The outermost layer of skin, the stratum corneum, has a role as the primary barrier against water evaporation from the body and drug entry through skin into the body. Thus, overcoming the stratum corneum barrier is important to develop transdermal drug delivery systems. Chemical approaches, such as penetration enhancers[1)]and physical approaches, such as iontophoresis[2)], phonophoresis[3)], and electroporation[4, 5)], have been evaluated to increase the skin permeation of several drugs. Physical approaches are often associated with several disadvantages, such as their requirement for special applica-

*Correspondence to: Kenji Sugibayashi, Faculty of Pharmaceutical Sciences, Josai University, 1-1 Keyakidai, Sakado, Saitama 350-0295, JAPAN
E-mail: sugib@josai.ac.jp
Accepted December 29, 2016 (received for review October 18, 2016)
Journal of Oleo Science ISSN 1345-8957 print / ISSN 1347-3352 online
http://www.jstage.jst.go.jp/browse/jos/ http://mc.manusriptcentral.com/jjocs

tion apparatus and their cost. Therefore, in the present study we aimed to evaluate the chemical or formulation approach with skin permeation-enhancing ability using a liquid crystal (LC) formulation. LCs are semisolids made of lipids with crystalline structures combining the properties of both crystal and liquid states. Glycerol monoolate (GMO) (Fig. 1) is one of the most widely studied LC-forming lipids used for topical application, and it is considered the gold standard for developing LC formulations[6, 7]. In the present study, we investigated the skin penetration enhancing effect of a novel LC-forming lipid, C_{17}-monoglycerol ester (MGE) (Fig. 1), and the results obtained were compared with those with GMO. Although previous studies have provided information on LC formulations for transdermal drug delivery[8, 9], very few studies have focused on the skin penetration-enhancing ability of LC-forming lipids with different physiochemical properties of drugs.

GMO is a very well-known self-assembling amphiphilic molecules that form a variety of crystalline structures with useful mechanical properties of special interest in drug delivery. In the presence of a small amount of water, GMO forms reversed micelles characterized by an oily texture[10]. As more water is added, a mucous-like system is formed that corresponds to the lamellar phase. GMO forms cubic or hexagonal phases when more water is added (20-40%) over a wide temperature range. These phases are highly viscous, in the presence of high amounts of water in temperatures ranging from 20-70℃, the cubic and hexagonal phases might exist in a stable condition[11, 12]. Previous research has demonstrated that the LC phases of GMO such as the cubic and hexagonal phases, increased transdermal drug delivery. As a transdermal absorption enhancer, GMO probably acts by causing a temporary and reversible disruption of the lamellar structure of the lipid bilayer in the stratum corneum and, in this way, increasing intercellular lipid fluidity[13].

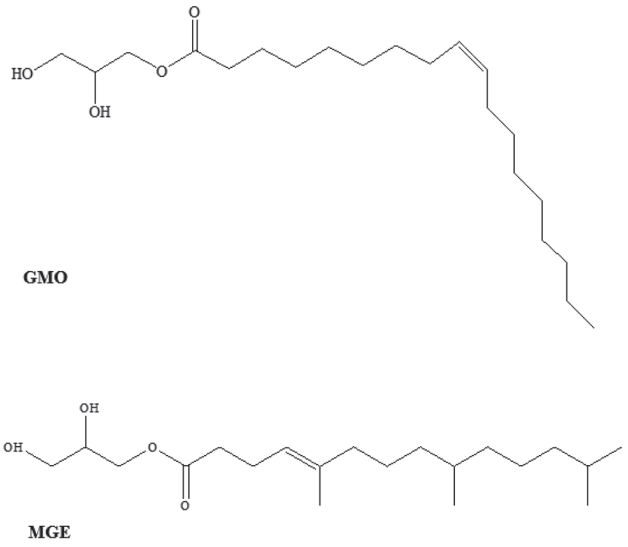

Fig. 1 Chemical structures of C_{17}-monoglycerol ester (MGE) and glyceryl monooleate (GMO).

In general, LCs can be classified into two categories, i.e., thermotropic and lyotropic. Thermotropic LCs are formed by a change in temperature, whereas lyotropic phases are obtained when mixed with several solvents. Lyotropic LCs usually consist of amphiphilic substances such as surfactants and solvents. Amphiphilic substances become micelles at a low concentration, consisting of a cluster of molecules with their polar groups oriented in water. This is a liquid isotropic phase, where isotropic means identical properties of the structure in all directions. More ordered structures such as lamellar, cubic, and hexagonal phases are formed with higher concentrations of lipids. These structures are formed because there is insufficient water to fill up spaces between the spherical or elongated micelles[14, 15]. Depending on the solvent concentration and the polarity of solvated mesogen, these systems can undergo phase transitions and structural modifications. Thus, their physiochemical and rheological properties can be systematically changed as required[16, 17]. Lyotropic LCs systems are spontaneously formed by various amphiphilic lipids such as GMO or phytantriol (PHT) in excess amounts of water with the presence of surfactants. Commonly encountered phases in lyotropic LCs include lamellar, cubic, and hexagonal phases[18, 19]. Among them, cubic and hexagonal phases have received much attention because of their highly ordered internal structures, and can be used as a slow release matrix for active pharmaceutical ingredients with various molecular sizes and polarities[20, 21].

Cubic and hexagonal LCs are often formed spontaneously by the addition of certain amphiphilic lipids in an aqueous environment[22]. When these LCs are dispersed into nanoparticles by the addition of excess water with stabilizers such as Pluronic copolymers and Myrj series[23, 24], they form stable colloidal dispersions that are termed cubosomes and hexosomes, respectively[25, 26]. Cubic bicontinuous phases have been identified, based on their surfaces: primitive (Im3m), diamond (Pn3m), and, most frequently, gyroid (Ia3d) bicontinuous LC phases. Hexagonal phases are formed by tubular aggregates and are either normal (H_1) or inverted (H_2) hexagonal LC phases.

In the present study, we initially prepared LC formulations containing drugs with different physiochemical properties (tranexamic acid [TXA], 4-methoxy-salicylic acid [4-MS], catechin [CC], and calcein [Cal]) (Table 1). These formulations were prepared using two different types of LC-forming lipids: MGE and GMO (Fig. 1). The chemical structures of MGE and GMO are showed in Fig. 1. As mentioned above, GMO is the most widely studied LC-forming lipid, but no previous studies have utilized the skin permeation enhancing ability of MGE.

The confirmation of LC phase structures in the prepared formulations was undertaken using a polarizing light micro-

Table 1 Physicochemical properties of the compounds used in the present study.

	Abbreviation	M.W.	log $K_{o/w}$*
Tranexamic acid	TXA	157.21	−0.3
4-Methoxy-salicylic acid	4-MS	152.14	0.5
Catechin	CC	290.26	0.8
Calcein	Cal	622.55	−2.02

* Octanol/water partition coefficient of compounds at pH 7.4

scope and small-angle X-ray scattering (SAXS). The physicochemical measurements of these formulations were performed using a viscometer and a Zetasizer. The release of drugs from LC formulations was determined using a dialysis release method. The skin penetration-enhancing ability of LC formulations was also investigated by *in vitro* skin permeation studies.

2 Materials and methods

2.1 Materials

MGE with a normal purity of >99.56% and GMO with a normal purity of >97% were obtained from Farnex Co., Inc. (Yokohama, Japan). TXA was purchased from Sigma Aldrich (St. Louis, MO, USA). 4-MS, CC, and Cal were purchased from Tokyo Chemical Industry Co., Ltd. (Tokyo, Japan). Other reagents and solvents were of special grade or HPLC grade and used without further purification.

2.2 Preparation of liquid crystalline formulation

Table 2 shows the composition of LC formulations prepared in this study. These formulations were designed based on a 1:1 ratio of the active ingredient in distilled water (drug solution) and LC-forming lipids. GMO was melted at 70℃ before use, but MGE was dispersed with drugs solution without preheating. The mixture was dispersed using a microsyringe dispenser (250 μL syringe) (Ito Corporation, Shizuka, Japan).

2.3 Polarizing light microscopic examination

The LC samples were observed using a polarizing light microscope (Olympus IX71, Tokyo, Japan). A pin-tip amount of the LC-forming lipid or LC formulation was smeared onto a microscope glass slide using a microsyringe dispenser and then quickly covered with a cover slip. The microsyringe containing LC-forming lipid or LC formulation was slowly pressed over the glass slide to make it as thin as possible. GMO was melted at 70℃ before pressing it over the glass slide, but MGE was pressed without preheating. A 40× objective lens and 10× eyepiece lens were used with cross polarizers in the bright field to detect birefringence. Micrographs was taken using the polarizing microscope.

2.4 Measurement of particle size and zeta potential

The particle size and zeta potential of LC formulations were determined using a dynamic light scattering Nano-ZS ZEN3600 Zetasizer (Malvern Instruments Ltd., Worcestershire, UK). LC samples were diluted in water and shaken using a vortex mixer prior to measurement. Following the particle size analysis of the LC formulations, the mode was switched from "Size" to "Zeta," and the zeta potential of the LC formulations was recorded. Each measurement for the particle size and zeta potential was repeated three times.

2.5 Measurement of viscosity

The viscosity of LC-formulations was measured using a viscometer (Toki Sangyo Co., Ltd., Tokyo, Japan) that allowed a sensitive determination of viscosity within a

Table 2 Composition of dispersed TXA-, 4-MS-, CC-, and Cal-LC formulations.

Formulation	Drug concentration	% Drug solution	% MGE	% GMO
TXA-MGE	19 mM	50	50	−
4-MS-MGE	1 mM	50	50	−
CC-MGE	10 mM	50	50	−
Cal-MGE	3 mM	50	50	−
TXA-GMO	19 mM	50	−	50
4-MS-GMO	1 mM	50	−	50
CC-GMO	10 mM	50	−	50
Cal-GMO	3 mM	50	−	50

range of 0.3–10,000 mPa·s with an accuracy of 1% relative error.

2.6 SAXS measurement

SAXS measurement of LC-formulations was performed using a Nano-Viewer (Rigaku, Tokyo, Japan) with a Pilatus 100K/RL 2D detector. The X-ray source was Cu Kα radiation with a wavelength of 1.54 Å and operating at 45 kV and 110 mA. The sample-to-detector distance was set at 375 mm. Each sample was placed into a vacuum-resistant glass capillary cell and exposed at 25℃ for 10 min. The SAXS pattern obtained was plotted against the scattering vector length, $q = (4\pi/\lambda)\sin(\theta/2)$, where θ is the scattering angle.

2.7 Release study

A dialysis membrane (molecular weight cut-off; 2,000–14,000 Da) (Sanko Junyaku Co., Tokyo, Japan) was set in a vertical-type diffusion cell (effective diffusion area: 0.95 cm^2) and the receiver chamber was maintained at 32℃. Phosphate-buffered saline (PBS; pH 7.4) was applied to the receiver chamber for TXA, 4-MS, and CC, and PBS containing 1.0 mM EDTA·2Na was used for Cal. Drug solution (1.0 mL) or its LC formulation (300 mg) was applied to the donor cell to start the release experiment. An aliquot (500 μL) was withdrawn from the receiver chamber, and the same volume of PBS or 1.0 mM EDTA·2Na was added to the chamber to keep the volume constant. The amount of TXA, 4-MS, and CC released was determined using an HPLC (Shimadzu Ltd., Kyoto, Japan). In case of Cal, the amount released was determined using a fluorescence spectrophotometer (Shimadzu Ltd., Kyoto, Japan). The cumulative % drug release was plotted against the square root of time (Higuchi's law)[27].

2.8 Animals

Male hairless rats (8 weeks old) were purchased either from Life Science Research Center, Josai University (Sakado, Saitama, Japan) or Ishikawa Experiment Animal Laboratories (Fukaya, Saitama, Japan). Animals were housed in temperature-controlled rooms (25 ± 2℃) with a 12 h light-dark cycle (07:00–19:00 h). The rats were allowed free access to food (Oriental Yeast Co., Tokyo, Japan) and tap water. The animal experiment protocol was approved by the Animal Care and Use Committee of Josai University (Sakado, Saitama, Japan).

2.9 *In vitro* skin permeation study

Full-thickness hairless rat skin was excised from the abdomen under anesthesia by *i.p.* injection of three types of anesthesia (medetomidine, 0.375 mg/kg; butorphanol, 2.5 mg/kg; and midazolam, 2 mg/kg). The excess fat was trimmed off and the skin samples were set in vertical-type diffusion cells (effective diffusion area: 0.95 cm^2) with the epidermis side facing the donor compartment. PBS (pH 7.4) with or without 1.0 mM EDTA·2Na was applied to the receiver chamber as in the release experiment and maintained at 32℃. These skin permeation experiments were conducted after hydration for 60 min with PBS with or without 1.0 mM EDTA·2Na. Drug solution (1.0 mL) or its LC-formulation (300 mg) was applied to the donor cell to start the *in vitro* skin permeation experiment. An aliquot (500 μL) was withdrawn from the receiver chamber, and the same volume of PBS with or without 1.0 mM EDTA·2Na was added to the chamber to keep the volume constant. The skin permeation of TXA, 4-MS, and CC was determined by HPLC, and that of Cal was determined using a fluorescence spectrophotometer.

2.10 HPLC conditions

The same volume of acetonitrile containing parabens was added to TXA, 4-MS, and CC samples. After gentle mixing, the sample was centrifuged for 5 min at 21,500 × g and 4℃ to remove proteins and contaminants. The supernatant was injected onto the HPLC. The HPLC system consisted of a pump (LC-10AD; Shimadzu, Kyoto, Japan), Chromatopac (C-R6A; Shimadzu), UV detector (SPD-6A; Shimadzu), system controller (SCL-6B; Shimadzu), and auto-injector (SIL-7A; Shimadzu). The LiChroCART®250-4 column (KGaA·64271; Merck, Darmstadt, Germany) was maintained at 40℃ during the eluting mobile phase, 0.1% phosphoric acid:acetonitrile = 75:25 for TXA, 0.1% phosphoric acid:acetonitrile = 55:45 for 4-MS, and 0.1% phosphoric acid containing 5 mM sodium dodecyl sulfate:acetonitrile = 50:50 for CC. The flow rate was adjusted to 1.0 mL/min. The injection volume was 20 μL, and detection was performed at 220 nm for TXA, 230 nm for 4-MS, and 245 nm for CC.

3 Results

3.1 Polarizing light microscopic examination

Figure 2 shows samples observed using a polarizing light microscope. No optical anisotropy was observed in cases of MGE and GMO alone (a, b) because these lipids cannot form crystalize structures without excess amount of water. In case of MGE- and GMO-LC formulations, they showed clear optical anisotropy on the displayed image (c, d, e, f, g, h, i, j). Moreover, these formulations appeared as uniform opaque ointment-like mixtures with no visible signs of aggregates.

In general, if there was any materials with high birefringence, the light output by the top layer, a linear polarizer, may cause optical anisotropy to appear on the displayed image, depending on the orientation of the viewer with respect to the display. These results showed that the present LC formulations were managed successfully to

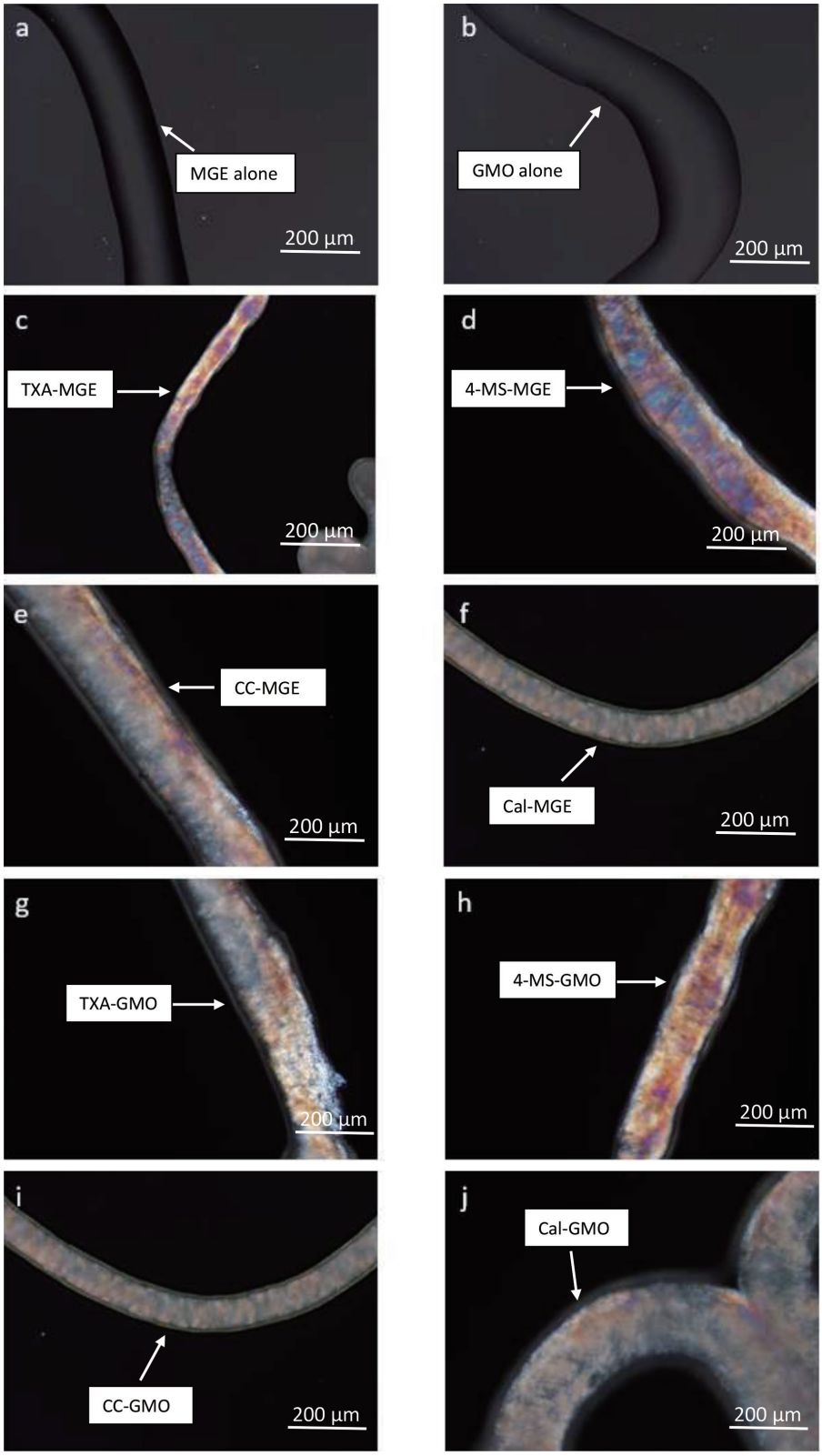

Fig. 2 LC-forming lipids or LC formulations upon application under polarized microscope: (a), MGE alone; (b), GMO alone; (c), TXA-MGE formulation; (d), 4-MS-MGE formulation; (e), CC-MGE formulation; (f), Cal-MGE formulation; (g), TXA-GMO formulation; (h), 4-MS-GMO formulation; (i), CC-GMO formulation and (j), Cal-GMO formulation. The optical anisotropy confirming the presence of LC in the prepared formulations.

form crystallized formulations because of high birefringence with the polarizing light microscope.

3.2 SAXS chart of LC formulations

The phase structure of TXA-, 4-MS-, and CC-MGE and GMO formulations was evaluated by SAXS. Figure 3 shows the X-ray diffraction profiles of all the formulations. The typical reflection patterns at nearly 1, $\sqrt{3}$, and $\sqrt{4}$ revealed the presence of a hexagonal phase (H_1, H_2) in all prepared formulations (a-d) (e-h in Supplementary data)[28, 29]. These results confirmed that both MGE- and GMO-LC formulations managed to form hexosomes successfully.

3.3 Measurement of particle size and zeta potential

The particle size and zeta potential of LC formulations were determined immediately (Fig. 4a, b) and 10 days (Fig. 4c, d in Supplementary data) after their preparation. The results showed that both MGE- and GMO-LC formulations had small particle sizes ranged between 220 and 280 nm, and the zeta potential of these formulations was ranged between −17 and −30 mV. In addition, no significant changes were observed in particle size or zeta potential at 10 days after their preparation.

3.4 Measurement of viscosity

The viscosity of LC formulations was measured using a viscometer. Figure 5 shows the obtained viscosity values. These values were affected dramatically by the type of LC-forming lipids used in the preparation. The viscosity values of LC formulations with MGE were significantly lower than those with GMO. These results showed that MGE-LC-formulations has lower viscosity than GMO-LC-formulations, and its low viscosity made it easy to handle and more practical for drug loading. GMO requires melting at 70℃ before its use for formulation preparation, but MGE was dispersed with drug solution without preheating owing to its low viscosity.

3.5 Drug release properties from LC formulations

The release study was performed using a vertical-type diffusion cell. Figure 6 shows the release profile of TXA, 4-MS, CC, and Cal from their MGE and GMO formulations. All profiles were obeyed to Higuchi's law[23]. The amounts of TXA, 4-MS, CC, and Cal released from MGE formulations were 13.9 ± 2.5%, 23.7 ± 3.2%, 16.7 ± 2.8%, and 9.6 ± 0.8%, respectively, against the initial dosing. In the case of GMO formulations, the amounts of TXA, 4-MS, CC, and Cal released were 7.3 ± 1.6%, 14.4 ± 2.2%, 10 ± 1.8%, and 6.1

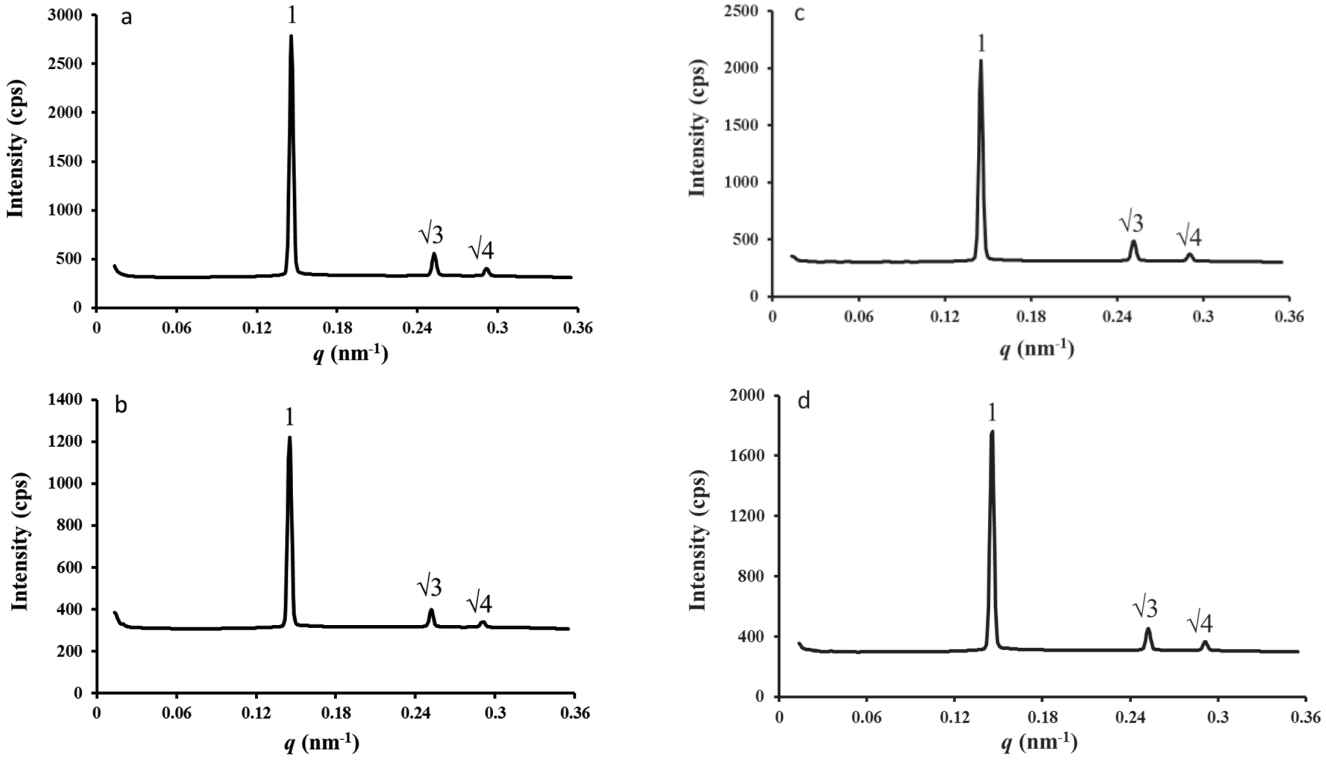

Fig. 3 SAXS charts of LC formulations.
(a), TXA-MGE formulation; (b), 4-MS-MGE formulation; (c), CC-MGE formulation; (d), Cal-MGE formulation; (e), TXA-GMO formulation; (f), 4-MS-GMO formulation; (g), CC-GMO formulation and (h), Cal-GMO formulation. The reflection patterns at: 1, $\sqrt{3}$, $\sqrt{4}$ confirming the presence of a hexagonal phase (H_1, H_2) for all prepared formulations (a-d) (e-h in Supplementary data).

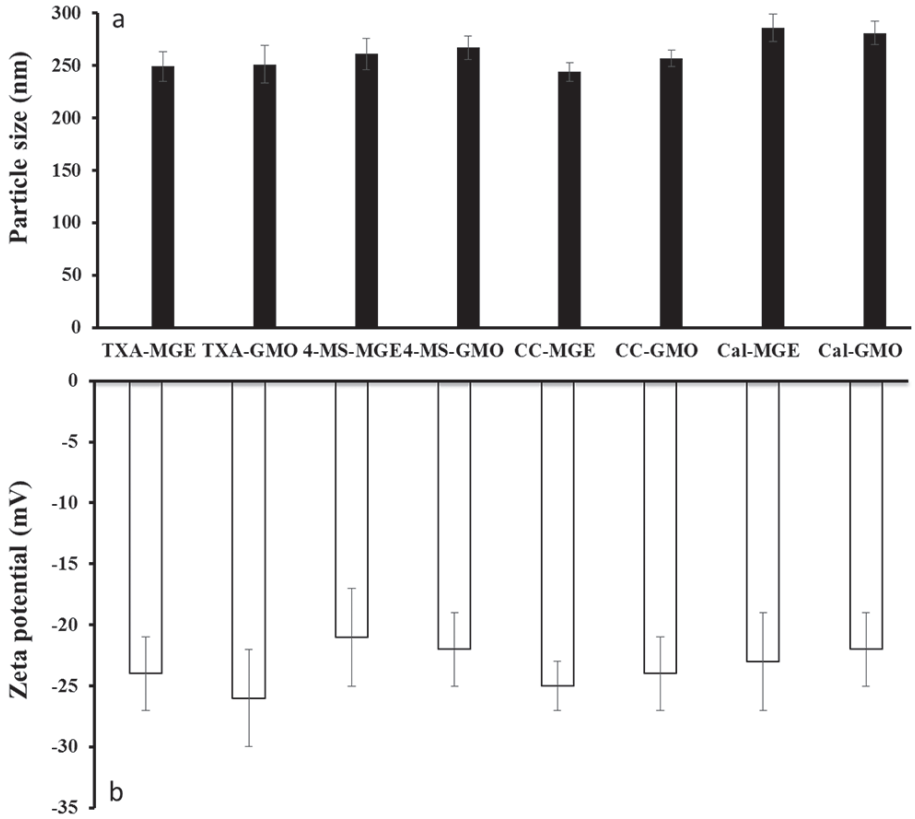

Fig. 4 Particle size (a, c) and zeta potential (b, d) of LC formulations immediately (a, b) and 10 days (c, d in Supplementary data) after preparation. Each point represents the mean ± S.E. of three experiments.

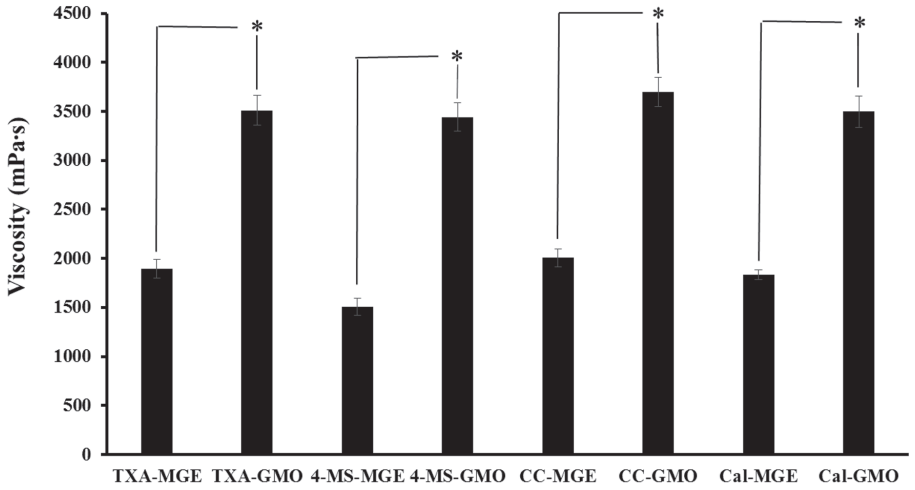

Fig. 5 The apparent viscosity of LC formulations.
Each point represents the mean ± S.E. of three experiments. *: $p<0.05$ significantly different from MGE-LC formulation (Student's t-test).

± 0.9%, respectively, against the initial dosing. These results might be related to the high viscosity of GMO-LC formulations and thus could affect the drug diffusivity and the release rate.

3.6 Skin permeation of drugs from LC formulations

Figure 7 shows the effect of MGE and GMO formulations on the time course of the cumulative amount of TXA, 4-MS, CC, and Cal that permeated through hairless rat intact skin. Significant improvements in skin permeation of TXA, 4-MS, and CC were observed after application their MGE

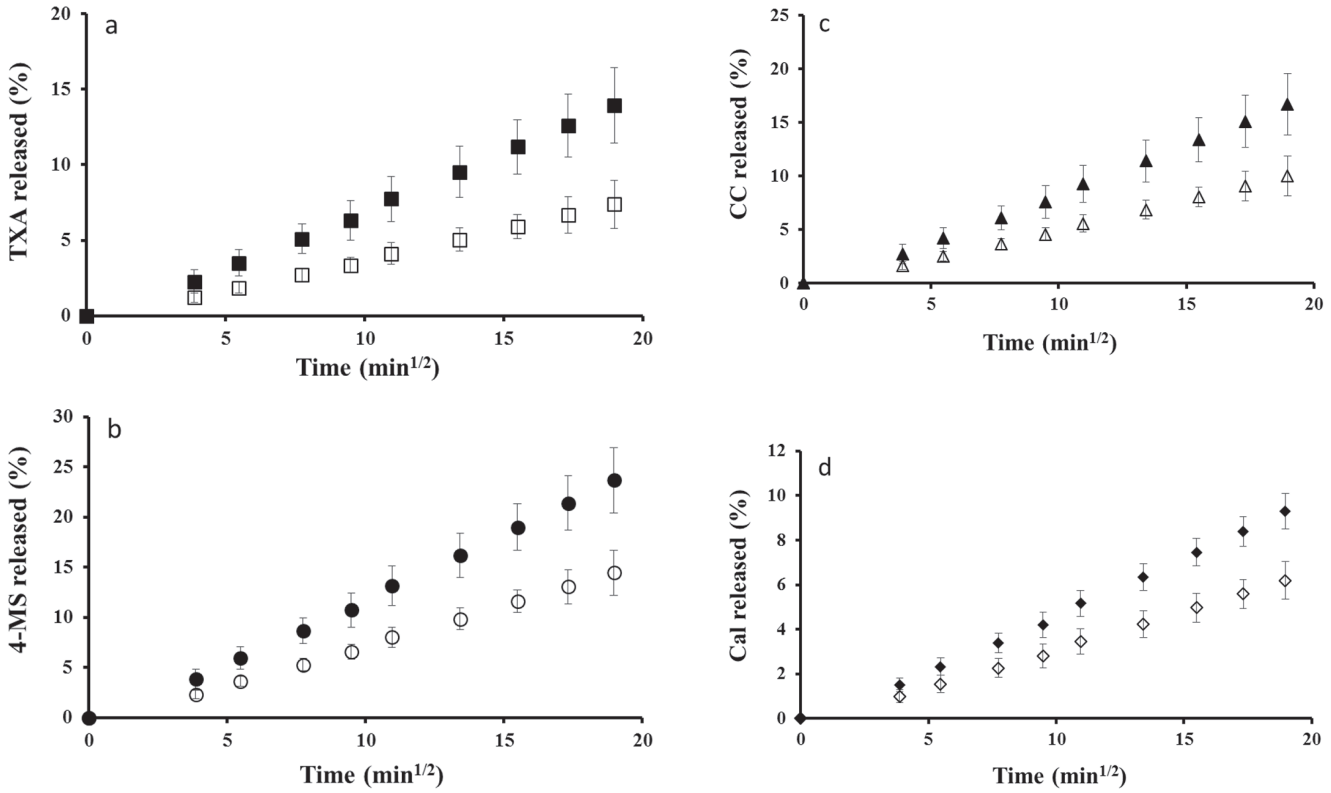

Fig. 6 Release profiles of TXA(a), 4-MS(b), CC(c)and Cal(d)from their LC formulations. Symbols: (a): (■), TXA-MGE formulation; (□), TXA-GMO formulation; (b): (●), 4-MS-MGE formulation; (○), 4-MS-GMO formulation; (c): (▲), CC-MGE formulation; (△)CC-GMO formulation; (d): (◆), Cal-MGE formulation; (◇), Cal-GMO formulation. Each point represents the mean ± S.E. of three experiments.

and GMO formulations compared with that permeated from drug solution(dissolved in water). The enhancement skin permeation ratios for TXA-, 4-MS-, CC-, and Cal-MGE formulations were 4.6, 3.5, 4.2, and 5.5, respectively, and those for TXA-, 4-MS-, CC-, and Cal-GMO formulations was 2.5, 2.6, 3.1, and 3, respectively. These results clearly showed that MGE formulations had better skin permeation enhancement effect compare with GMO formulations.

4 Discussion

LC-forming lipids represent an important class of biocompatible amphiphiles, and their application extends to several fields, such as cosmeceutical, dietary, and pharmaceutical technologies[30]. In recent years, the LC phases formed by LC-forming lipids have been shown to be able to accommodate biologically active molecules such as vitamins, enzymes, and other proteins[31–33]. This ability opens new possibilities for pharmaceutical applications. Previous researches have demonstrated that the LC phases, such as cubic and hexagonal phases, increased transdermal drug delivery[8, 34]. The advantages of LC formulations for transdermal drug delivery systems might include biocompatibility and the ability to self-assemble their structure[19].

In the present study, we investigated the usefulness of MGE-LC as a new skin permeation enhancing approach, and the obtained results were compared with GMO as one of the most widely studied LC-forming lipids used in topical formulations.

TXA, 4-MS and CC drug models were selected due to their topical therapeutic beneficial. Topical application of TXA to bleeding wound surfaces can reduce the blood loss. 4-MS can be used to treat skin conditions that involve scaling or overgrowth of skin cells such as psoriasis, ichthyoses, corns, calluses, and warts on the hands or feet. CC can inhibit skin tumorigenesis, reducing inflammation, protecting skin from UV-induced various damages and inhibiting formation of melanin. However, these drug models have low transdermal absorption[35, 36]. Moreover, Cal has low transdermal absorption because of its hydrophilicity and large molecular weight. Therefore, TXA, 4-MS, CC and Cal were selected as drug models for skin studies.

We prepared LC formulations using MGE and GMO containing drugs based on a 1:1 ratio, as shown in Table 2. These formulations were prepared by extruding lipid dispersion 50 times with a microsyringe dispenser, to incorporate high percentage of lipid(50%)with the drug solution

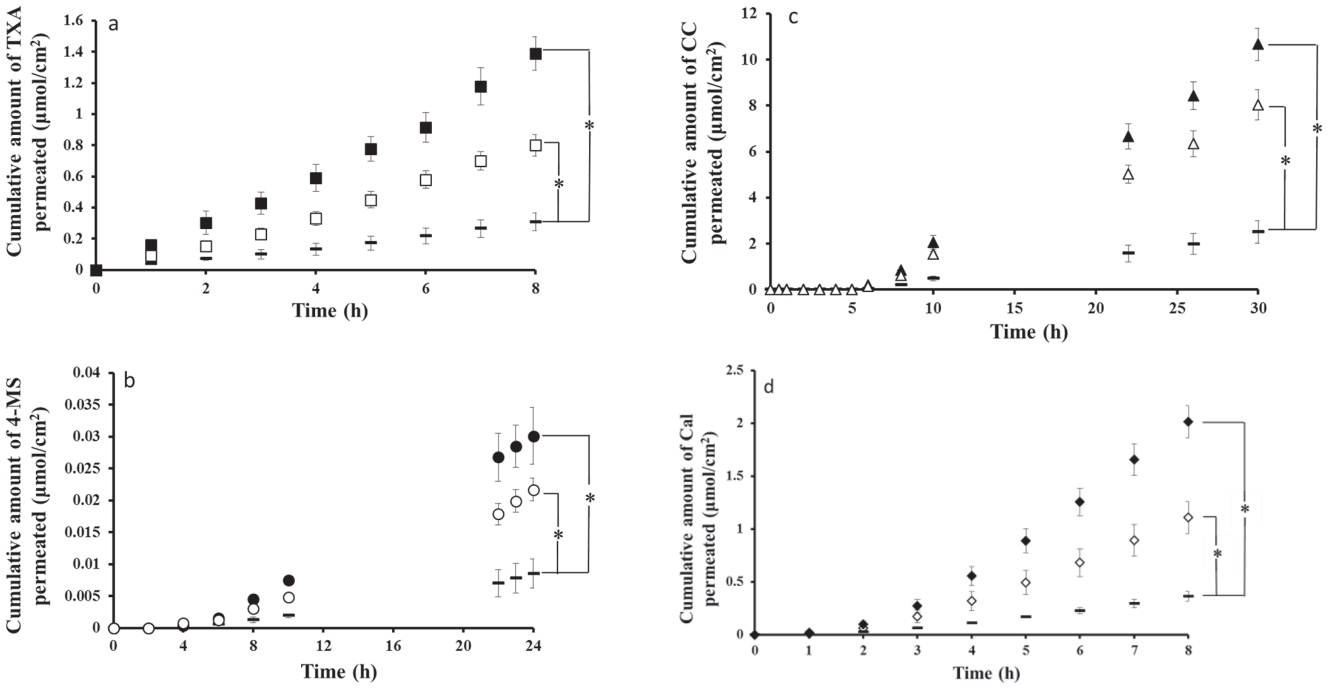

Fig. 7 Effect of LC formulation on the time course of the cumulative amount of TXA (a), 4-MS (b), CC (c) and Cal (d) that permeated through hairless rat intact skin.
Symbols: (a): (−), TXA solution; (■), TXA-MGE formulation; (□), TXA-GMO formulation; (b): (−), 4-MS solution; (●), 4-MS-MGE formulation; (○), 4-MS-GMO formulation; (c): (−), CC solution; (▲), CC-MGE formulation; (△) CC-GMO formulation; (d): (−), Cal solution; (◆), Cal-MGE formulation; (◇), Cal-GMO formulation. Each point represents the mean ± S.E. of three experiments. *: $p < 0.05$ significantly different from drug solution (Student's t-test).

(50%). This technique has an advantage by mixing high concentration of lipid up to 50% with the drug solution without the aid of dispersant. Non-uniform mixtures with high viscus aggregate were observed using other techniques such as homogenizer and ultrasonic even in the presence of dispersants.

Birefringence was investigated for the prepared formulations using a polarizing light microscope. As a result, TXA-, 4-MS-, CC-, and Cal-MGE and GMO formulations showed a clear optical anisotropy on the images (Fig. 2c-j); however, no optical anisotropy was observed in the case of MGE and GMO alone (Fig. 2a, b). These results strongly suggested that both MGE and GMO formulations managed to form crystalline formulations successfully because of the high birefringence of these formulations.

Furthermore, the phase structure of the formulations was examined by SAXS, and the results showed that typical reflection patterns at nearly 1, $\sqrt{3}$, and $\sqrt{4}$ for both MGE and GMO formulations revealed the presence of a hexagonal phase (H_1, H_2) (Fig. 3a-d) (Fig. 3e-h in Supplementary data). The driving force of forming hexosome systems is the physically applied shear stress by microsyringe dispensers.

The critical packing parameter (CPP) is useful in predicting which phases can be preferentially formed by a given lipid. When CPP <1, oil-in-water self-assembled structures form, such as normal micelles, normal cubic structure, and normal hexagonal phases. When CPP >1, water-in-oil self-assembled structures form, such as reversed micelles, reversed cubic structure, and reversed hexagonal structure[37]. Additives or active ingredients might affect CPP as well as the LC phase structure. Generally, GMO formed the invert-type LC with CPP >1[10]. No previous studies have performed on the effect of CPP on the LC phase structure formed by MGE.

Previous studies have reported that the hexagonal phase presents some advantages. It has a larger surface area to interact with the skin, high fluidity, and can be incorporated into compounds independently of their solubility[38, 39]. Although a hexagonal phase (H_1, H_2) was formed in all prepared formulations, factors such as concentration of lipid and drug could influence the phase transition of these formulations. Further studies are necessary to be conducted to understand the effect of such factors on the phase transition of LC formulations.

The particle size and zeta potential of MGE- and GMO-LC formulations were determined immediately (Fig. 4a, b) and at 10 days after preparation (Fig. 4c, d in Supple-

mentary data). The obtained data showed that these formulations had small particle size (220-280 nm) and the zeta potential ranged between −17 and −30 mV. In addition, no significant changes were observed in the particle size or zeta potential measurements at 10 days after preparation. These results suggested that the present MGE and GMO formulations had small particle size with high surface charges and electrical repulsion between the particles, and thus their aggregation was prevented even 10 days after preparation. The zeta potential present strong negative values for all the analyzed samples, indicating the predominance of repulsive forces. The reason why LC formulations showed negative zeta potential values is due to the present of free oleic acid in the lipid phase may give rise to the negative charge of the particles. In addition, the negative charge can also be explained by preferential adsorption of hydroxyl ions at the lipid-water interface.

These results were consistent with previous findings on the zeta optional of LC formulations[40].

Furthermore, the viscosity of the formulations was measured. The viscosity of LC formulations with MGE was significantly lower than those with GMO. In contrast to MGE, the high viscosity of GMO makes it less easy to handle, impractical for drug loading, and requires melting at 70℃ before use. These results suggested that the type of LC-forming lipid dramatically affected the viscosity of the formulation (Fig. 5). In consequence, the drug release results showed that the low viscosity of MGE-LC-formulations could influence the drug diffusivity and the release rate of the entrapped drugs in its formulations (Fig. 6). In general, hydrophilic drugs tend to be located close to the polar head of lipid or in the water channels (water phase), whereas lipophilic drugs will be loaded in the lipid bilayer and amphiphilic drugs in the interface (lipid phase). The aqueous and lipid phase in our formulation design were in a ratio 1:1, therefore, these formulations can accommodate a wide range of different physiochemical drugs. The obtained release profiles suggest that the viscosity of hexagonal is the decisive factor that mainly influenced of drug diffusion in LC-formulations. The low viscosity of MGE could be related to the chained-liked terpenes and double bound in its structure (Fig. 1).

In vitro skin permeation experiment was carried out using hairless rat skin. Correlation of skin permeation of chemicals to human skin is very important, previous studies showed a good relationships of skin permeation of chemicals between human and hairless rat skin[41, 42]. Significant improvement in the skin permeation of different drugs was observed after application of MGE and GMO formulations (Fig. 7). The enhancement of the skin permeation ratio of MGE formulations was higher than those of GMO formulations. These results clearly showed that MGE formulations managed to improve the skin permeation enhancement effect compared with GMO formulations. These findings could be related to the low viscosity of MGE formulations, and this might offer better drug diffusivity and influence the movement and permeation of the drugs in and across the skin. The detailed mechanism of the skin permeation enhancing ability by LC systems is not fully understood[43]. It was speculated that cubic structure with similar nano-structure as the skin, increases the interaction between skin and formulation and enhances the skin permeation[44, 45]. A previous study[46] reported that the hexagonal phase may facilitate the fusion of LCs with the stratum corneum and deeper skin layers and thereby may improve drug delivery to the skin. Moreover, the hexosome system, owing to its larger surface area to interact with the skin and high fluidity, can be incorporated into compounds independently of their solubility[38, 39]. Further studies are needed to clarify the mechanism and effect of LC phase structure on the skin permeation of drugs.

5 Conclusion

The present study confirmed that both MGE- and GMO-LC-forming lipids shared the same behavior in terms of their birefringence index, LC phase structure, particle size, and zeta potential. Both the MGE- and GMO-LC formulations managed to improve skin permeation of various physiochemical properties of the drugs. However, MGE formulations had lower viscosity, faster drug release, and better skin permeation than GMO formulations. Our results strongly suggested that the low viscosity of MGE-LC-formulations might influence drug diffusivity and permeability through skin. The present MGE-LC forming lipid can be utilized as a promising new topical formulation for therapeutic drugs and cosmetic ingredients.

Supporting Information

This material is available free of charge via the Internet at http://dx.doi.org/jos.66.10.5650/jos.ess.16204

References

1) Purdon, C.H.; Azzi, C.G.; Zhang, J.; Smith, E.W.; Maibach, H.I. Penetration enhancement of transdermal delivery-current permutations and limitations. *Crit. Rev. Ther. Drug Carrier Syst.* **21**, 97-132 (2004).
2) Kasha, P.C.; Banga, A.K. A review of patent literature for iontophoretic delivery and devices. *Recent Pat. Drug Deliv. Formul.* **2**, 41-50 (2008).
3) Ogura, M.; Paliwal, S.; Mitragotri S. Low-frequency sonophoresis: current status and future prospects. *Adv. Drug Deliv. Rev.* **60**, 1218-1223 (2008).

4) Tokumoto, S.; Mori, K.; Higo, N.; Sugibayashi, K. Effect of electroporation on the electroosmosis across hairless mouse skin in vitro. *J. Control. Release* **105**, 296-304 (2005).
5) Tokudome, Y.; Sugibayashi, K. Mechanism of the synergic effects of calcium chloride and electroporation on the in vitro enhanced skin permeation of drugs. *J. Control. Release* **95**, 267-274 (2004).
6) Larsson, K. Aqueous dispersions of cubic lipid–water phases. *Curr. Opin. Colloid In.* **5**, 64-69 (2000).
7) Caboi, F.; Amico, G.S.; Pitzalis, P.; Monduzzi, M.; Nylander, T.; Larsson, K. Addition of hydrophilic and lipophilic compounds of biological relevance to the monoolein/water system. I. Phase behavior. *Chem. Phys. Lipids* **109**, 47-62 (2001).
8) Yamada, K.; Yamashita, J.; Todo, H.; Miyamoto, K.; Hashimoto, S.; Tokudome, Y.; Hashimoto, F.; Sugibayashi, K. Preparation and evaluation of liquid crystal formulation having skin permeation- enhancing ability of the entrapped drug. *J. Oleo Sci.* **60**, 31-40 (2011).
9) Dae, G.L.; Won, W.J.; Nam, A.K.; Jun, Y.L.; Seol, H.L.; Woo, S.S.; Nae, G.K.; Seong, H.J. Effect of the glyceryl monooleate-based lyotropic phases on skin permeation using in vitro diffusion and skin imaging. *Asian J. Pharm. Sci.* **9**, 324-329 (2014).
10) Chen, Y.; Ma, P.; Gui, S. Cubic and hexagonal liquid crystals as drug delivery systems. *Biomed. Res. Int.* **2014**, http://dx.doi.org/10.1155/2014/815981 (2014).
11) Biltonen, R.L.; Lichtenberg, D. The use of differential scanning calorimetry as a tool to characterize liposome preparations. *Chem. Phys. Lipids* **64**, 128-142 (1993).
12) Ganem-Quintanar, A.; Quintanar-Guerrero, D.; Buri, P. Monoolein: a review of the pharmaceutical applications. *Drug Dev. Ind. Pharm.* **26**, 809-820 (2000).
13) Bode, J.C.; Kuntsche, J.; Funari, S.S.; Bunjes, H. Interaction of dispersed cubic phases with blood components. *Int. J. Pharm.* **448**, 87-95 (2013).
14) Guo, C.; Wang, J.; Cao, F., Lee, R.J.; Zhai, G. Lyotropic liquid crystal systems in drug delivery. *Drug Discov. Today* **15**, 1032-1040 (2010).
15) Siddig, M.A.; Radiman, S.; Muniandy, S.V.; Jan, L.S. Structure of cubic phases in ternary systems glucopone/water/hydrocarbon. *Colloids Surf. A Physicochem. Eng. Asp.* **236**, 57-67 (2004).
16) Makai, M.; Csanyi, E.; Nemeth, Z.; Palinkas, J.; Eros, I. Structure and drug release of lamellar liquid crystals containing glycerol. *Int. J. Pharm.* **256**, 95-107 (2003).
17) Fong, W.K.; Hanley, T.; Boyd, B.J. Stimuli responsive liquid crystals provide 'on-demand' drug delivery *in vitro* and *in vivo*. *J. Control. Release* **135**, 218-226 (2009).
18) Clogston, J.; Rathman, J.; Tomasko, D.; Walker, H.; Caffrey, M. Phase behavior of a monoacylglycerol: (myverol 18-99 K)/water system. *Chem. Phys. Lipids* **107**, 191-220 (2000).
19) Kadhum, W.R.; Todo, H.; Sugibayashi, K. Skin permeation: Enhancing ability of liquid crystal formulations. in *Percutaneous penetration enhancers chemical methods in penetration enhancement: Drug Manipulation Strategies and Vehicle Effects* (Dragicevic-Curic, N.; Maibach, H. eds.). Springer-Verlag, Berlin Heidelberg, pp. 243-253 (2015).
20) Drummond, C.J.; Fong, C. Surfactant self-assembly objects as novel drug delivery vehicles. *Curr. Opin. Colloid Interface Sci.* **4**, 449-456 (1999).
21) Shah, J.C.; Sadhale, Y.; Chilukuri, D.M. Cubic phase gels as drug delivery systems. *Adv. Drug Deliv. Rev.* **47**, 229-250 (2001).
22) Kaasgaard, T.; Drummond, C.J. Ordered 2-D and 3-D nanostructured amphiphile self-assembly materials stable in excess solvent. *Phys. Chem. Chem. Phys.* **8**, 4957-4975 (2006).
23) Kadhum, W.R.; Oshizaka, T.; Hijikuro, I.; Todo, H.; Sugibayashi, K. Usefulness of liquid–crystal oral formulations to enhance the bioavailability and skin tissue targeting of p-amino benzoic acid as a model compound. *Eur. J. Pharm. Sci.* **88**, 282-290 (2016).
24) Chong, J.Y.T.; Mulet, X.; Waddington, L.J.; Boyd, B.J.; Drummond C.J. High-throughput discovery of novel steric stabilizers for cubic lyotropic liquid crystal nanoparticle dispersions. *Langmuir* **28**, 9223-9232 (2012).
25) Spicer, P.T. Progress in liquid crystalline dispersions: cubosomes. *Curr. Opin. Colloid Interface Sci.* **10**, 274-279 (2005).
26) Yaghmur, A.; Glatter, O. Characterization and potential applications of nanostructured aqueous dispersions. *Adv. Colloid Interface Sci.* **148**, 333-342 (2009).
27) Higuchi, T. Mechanism of sustained action medication: theoretical analysis of rate of release of solid drugs dispersed in solid matrices. *J. Pharm. Sci.* **52**, 1145-1148 (1963).
28) Anderson, D.M.; Gruner, S.M.; Leibler, S. Geometrical aspects of the frustration in the cubic phases of lyotropic liquid crystals. *Proc. Natl. Acad. Sci. USA* **85**, 5364-5368 (1988).
29) Qiu, H.; Caffrey, M. The phase diagram of monoolein/water system: metastability and equilibrium aspects. *Biomaterials* **21**, 223-234 (2000).
30) Ericsson, B.; Eriksson, P.O.; Lofroth, J.E.; Engstrom, S. Cubic phases as delivery systems for peptide drugs. *ACS Symp. Ser.* **469**, 252-263 (1991).
31) Wallin, R.; Engstrom, S.; Mandenius, C.F. Stabilisation of glucose oxidase by entrapment in a cubic liquid crystalline phase. *Biocatalysis* **8**, 73-80 (1993).

32) Nylander, T.; Mattisson, C.; Razumas, V.; Miezes, Y.; Hakansson, B. A study of entrapped enzyme stability and substrate diffusion in a monoglyceride-based cubic liquid crystalline phase. *Colloids Surf. A.* **114**, 311-320(1996).
33) Caboi, F.; Nylander, T.; Razumas, V.; Talaikyte, Z.; Monduzzi, M.; Larsson, K. Structural effects, mobility, and redox behavior of vitamin K1 hosted in the monoolein:water liquid crystalline phases. *Langmuir* **13**, 5476-5483(1997).
34) Lopes, L.B.; Speretta, F.F.; Bentley, M. Enhancement of skin penetration of vitamin K using monooleinbased liquid crystalline systems. *Eur. J. Pharm. Sci.* **32**, 209-215(2007).
35) Wong, J.; Abrishami, A.; El Beheiry, H.; Mahomed, N.N.; Roderick D.J.; Gandhi, R.; Syed, K.A.; Muhammad, O.H.S.; De Silva, Y.; Chung, F. Topical application of tranexamic acid reduces postoperative blood loss in total knee arthroplasty: a randomized, controlled trial. *J. Bone Joint Surg. Am.* **15**, 2503-2513(2010).
36) Wada, Y.; Ishii, F. Potential power of green tea catechins. *J. Oleo Sci.* **8**, 371-378(2008).
37) Guo, C.; Wang, J.; Cao, F.; Lee, R.J.; Zhai, G. Lyotropic liquid crystal systems in drug delivery. *Drug Discov. Today* **15**, 1032-1040(2010).
38) Siekmann, B.; Bunjes, H.; Koch, M.H.J.; Westesen, K. Preparation and structural investigations of colloidal dispersions prepared from cubic monoglyceride-water phases. *Int. J. Pharm.* **244**, 33-43(2002).
39) Esposito, E.; Eblovi, N.; Rasi, S.; Drechsler, M.; Di Gregorio, G.; Menegatti, E.; Cortesi, R. Lipid-based supramolecular systems for topical application: a preformulatory study. *AAPS PharmSciTech.* **5**, 1-15(2003).
40) Sherif, S.; Bendas, E.R.; Badawy, S. The clinical efficacy of cosmeceutical application of liquid crystalline nanostructured dispersions of alpha lipoic acid as antiwrinkle. *Eur. J. Pharm. Biopharm.* **86**, 251-259 (2014).
41) Watanabe, T.; Hasegawa, T.; Takahashi, H.; Ishibashi, T.; Takayama, K.; Sugibayshi, K. Utility of the three-dimensional cultured human skin model as a tool to evaluate skin permeation of drugs. *AATEX* **8**, 1-14 (2001).
42) Morimoto, Y.; Hatanaka, T.; Sugibayashi, K.; Omiya, H. Prediction of skin permeability of drugs: comparison of human and hairless rat skin. *J. Pharm. Pharmacol.* **44**, 634-639(1992).
43) Uchino, T.; Murata, A.; Miyazaki, Y.; Oka, T.; Kagawa, Y. Glyceryl monooleyl ether-based liquid crystalline nanoparticles as a transdermal delivery system of flurbiprofen: characterization and *in vitro* transport. *Chem. Pharm. Bull.* **63**, 334-340(2015).
44) Esposito, E.; Cortesi, R.; Drechsler, M.; Paccamiccio, L.; Mariani, P.; Contado, C.; Stellin, E.; Menegatti, E.; Bonina, F.; Puglia, C. Cubosome dispersions as delivery systems for percutaneous administration of indomethacin. *Pharm. Res.* **22**, 2163-2173(2005).
45) Evenbratt, H.; Jonsson, C.; Faergemann, J.; Engstrom, S.; Ericson, M.B. *In vivo* study of an instantly formed lipid–water cubic phase formulation for efficient topical delivery of aminolevulinic acid and methyl-aminolevulinate. *Int. J. Pharm.* **452**, 270-275(2013).
46) Lopes, L.B.; Ferreira, D.A.; de Paula, D.; Garcia, M.T.; Thomazini, J.A.; Fantini, M.C.; Bentley, M.V. Reverse hexagonal phase nanodispersion of monoolein and oleic acid for topical delivery of peptides: in vitro and in vivo skin penetration of cyclosporin *A. Pharm. Res.* **23**, 1332-1342(2006).